

Magnetization Process of One-Dimensional Quantum Antiferromagnet: The Product Wavefunction Renormalization Group Approach

Yasuhiro Hieida, Kouichi Okunishi, and Yasuhiro Akutsu

January 31, 1997

*Department of Physics, Graduate School of Science, Osaka University,
Machikaneyama-cho 1-1, Toyonaka, Osaka 560, Japan*

Abstract

The product-wavefunction renormalization group method, which is a novel numerical renormalization group scheme proposed recently, is applied to one-dimensional quantum spin chains in a magnetic field. We draw the zero-temperature magnetization curve of the spin chains, which excellently agrees with the exact solution in the whole range of the field.

PACS codes: 02.70.-c, 05.30.-d, 75.10.Jm, 75.30.Kz

Key Words: quantum spin chain, numerical renormalization, magnetization curve

Address: Yasuhiro Hieida c/o Yasuhiro Akutsu

Department of Physics, Graduate School of Science,

Osaka University, Toyonaka, Osaka 560, JAPAN

Phone: +81-6-850-5349, **Fax:** +81-6-845-0518

e-mail: hieida@godzilla.phys.sci.osaka-u.ac.jp

Many interesting problems which have been left unsolved mostly concerned with strongly correlated systems where many-body effects play essential roles. For these problems conventional many-body-theoretic techniques, e.g., the mean-field approximation and the perturbation expansion, lose their power; these methods often fail in explaining even qualitative features of the system. As promising substitutes, we have direct numerical approaches which are rapidly developing in accordance with the remarkable advancement of the computer technology. Examples are the Monte-Carlo simulation, the molecular dynamics and the exact diagonalization of Hamiltonian matrices or transfer matrices, which have been successfully applied to various problems.

In these direct numerical methods we face another problem: Since the system size N (number of lattice points, for example) which we can deal with is always finite, we need extrapolation with respect to N to extract the behavior in the thermodynamic limit ($N \rightarrow \infty$). As a standard prescription we have the finite-size scaling method [1], which has been one of most successful extrapolation schemes for studying the critical phenomena. In applying the finite-size scaling, we must compute the N -dependence of physical quantities for large enough N , which often requires long computation time. For the exact diagonalization method, the large- N problem is rather serious due to the exponential growth of the Hamiltonian matrix dimension, which imposes severe limitation on feasible system size N .

The density-matrix renormalization group (DMRG) method invented by S. R. White is a very important step to overcome the large- N difficulty. The method was introduced as an approximate diagonalization scheme and has been applied to one-dimensional quantum systems, with results demonstrating surprising efficiency of the method [2]. The method is also applicable to two-dimensional lattice statistical models for diagonalization the transfer matrices instead of the Hamiltonian matrices [3].

Quite recently, two novel algorithms are devised by T. Nishino and K. Okunishi, which are closely connected to the DMRG. One is the corner-transfer-matrix renormalization group (CTMRG) method [4, 5] and the other is the product-wave-function renormalization group (PWFRG) method [6]. In the CTMRG, a systematic renormalization scheme for large-lattice-size two-dimensional classical spin systems is given in terms of Baxter's corner transfer matrix [7]. In the PWFRG, one diagonalizes the "wavefunction matrix" instead of the density matrix to obtain the "projection matrix" for retained block-state bases and sets up a recursion relation for the "projection matrix". As has been shown in refs [4, 5, 6]. both methods are highly effi-

cient for 2D classical systems. Hence, if we can extend them to 1D quantum systems, similar efficiency may be expected. For 1D quantum systems, the PWFRG seems to be more easily implemented than the CTMRG, because the latter takes full advantage of the two-dimensionality of the system. The actual implementation, however, is non-trivial because the transfer-matrix multiplication employed in the original PWFRG lose meaning for quantum systems.

The aim of this article is to show that the PWFRG can actually be extended to quantum systems and to demonstrate the efficiency of the “quantum PWFRG” by applying it to 1D quantum antiferromagnets in the uniform magnetic field to obtain the magnetization curve at zero temperature. The importance of the study of the magnetization curve itself is clear. First, the magnetization process or M (magnetization)- H (magnetic field) curve is a directly and accurately observable quantity by experiments [8, 9]. We need reliable theoretical calculation on various models for comparison with experiments. Second, a magnetized state which is the lowest energy state for $H > H_c$ (H_c : lower critical field), is an excited state at $H = 0$. This means that the magnetization curve contains a considerable amount of information about the whole energy-level structure of the system. Third, for gapless systems, the efficiency (or inefficiency) of the numerical renormalization groups like the DMRG and the PWFRG has not been fully tested yet. Calculations of the magnetization curve would also serve as this test, because the finitely-magnetized ground states of Heisenberg-like quantum antiferromagnets are gapless states.

Consider a spin- S antiferromagnetic spin chain in a field whose Hamiltonian \mathcal{H} is expressed as

$$\mathcal{H} = \sum_i h(\vec{s}_i, \vec{s}_{i+1}) - H \sum_i s_i^z \quad (1)$$

where \vec{s}_i is the spin operator at the site i and h is the nearest-neighbor coupling function (or *local Hamiltonian*). We take a unit where $g\mu_B = 1$ (g : g -factor, μ_B : Bohr magneton) or these factors are absorbed into the field H . The “pure” Heisenberg model corresponds to $h = h(\vec{s}_i, \vec{s}_{i+1}) = -J\vec{s}_i \cdot \vec{s}_{i+1}$ (J : an exchange coupling constant), but we consider more general form of h conserving the total S^z . Our problem is to find the lowest energy state of \mathcal{H} .

Let us briefly explain the PWFRG which is a close relative of the DMRG. Recall the infinite-system algorithm of the DMRG [2]. Write the ground-state wave function for $2N$ -site system under the free boundary condition,

obtained by diagonalizing the Hamiltonian matrix, as

$$\Psi_G^{2N}(\alpha|\beta) \quad (2)$$

where α (resp. β) is the block-state index for the left-half (resp. right-half) N sites. For simplicity, we restrict ourselves to the cases where \mathcal{H} is mirror symmetric and the ground-state wavefunction is of even parity with respect to the space reflection. If we extend the system by adding two sites at the center of the system, the ground-state wavefunction of the two-site extended system (with the extended Hamiltonian) can be written as

$$\Psi_G^{2N+2}(\alpha, i|j, \beta) \quad (3)$$

where i and j denote spin states (e.g., $i = -S, -S + 1, \dots, S$ in the S^z -diagonal representation) for added sites. In the DMRG, we form the density matrix ρ as

$$\rho(i', \alpha'|i, \alpha) = \sum_{j, \beta} \Psi_G^{2N+2}(\alpha', i'|j, \beta) \Psi_G^{2N+2}(\alpha, i|j, \beta) \quad (4)$$

and diagonalize it to choose m eigenstates with eigenvalues λ_μ ($\mu = 1, 2, \dots, m$, in descending order in magnitude). We retain the m eigenstates as new block states (bases) forming a truncated basis set for $(N + 1)$ -site system. These two, (P1) the diagonalization of \mathcal{H} for the extended system, and (P2) the choice of retained bases through the density-matrix diagonalization, are the key processes in the DMRG.

In the PWFRG, these key processes are changed as follows. The process (P1) is replaced by, (P1') the *improvement* of the “input” wavefunction. In 2D classical systems for which the original PWFRG is developed, the improvement is made by the multiplication of the transfer matrix [6]. For 1D quantum systems, the transfer-matrix multiplication is successfully substituted by the modified Lanczos operation [10, 11] on the wavefunction (see eq.(9) below). As for the process (P2), the diagonalization of the density matrix is replaced by, (P2') diagonalization of the “wavefunction matrix” $\hat{\Psi}$:

$$\hat{\Psi}(\alpha, i|\beta, j) = \Psi_G(\alpha, i|j, \beta), \quad (5)$$

where we have suppressed the superscript denoting the number of lattice sites. In terms of the “projection matrix” $R(\alpha, i|\mu)$ which projects the state (α, i) into the new block state μ , we have

$$\hat{\Psi}(\alpha, i|\beta, j) = \sum_{\mu} R(\alpha, i|\mu) \omega_{\mu} R(\beta, j|\mu). \quad (6)$$

Since $\rho = \hat{\Psi}^2$, the density-matrix eigenvalues $\{\lambda_\mu\}$ relate to the wavefunction-matrix eigenvalues $\{\omega_\mu\}$ as $\lambda_\mu = \omega_\mu^2$ [6]. Hence the choice of retained bases according to the magnitude of $|\omega_\mu|$ is equivalent to that made in the DMRG. As in the DMRG, the projection matrix R is also used in the construction of the new block Hamiltonian for the size-extended system.

There is one important process added in the PWFRG: (P3') We set up a recursion relation for R as follows. By $A(\alpha, i|\mu)$ we denote the “refined” projection matrix associated with the improved wavefunction obtained by the process (P1'). The recursion relation reads [6]

$$R_{\text{new}}(\alpha, i|\mu) = \sum_{j, \eta, \xi} A(\xi, j|\alpha) R_{\text{old}}(\xi, j|\eta) A(\eta, i|\mu). \quad (7)$$

Updated wavefunction matrix is then given by

$$\hat{\Psi}_{\text{new}}(\alpha, i|\beta, j) = \sum_{\mu} R_{\text{new}}(\alpha, i|\mu) \omega_{\mu} R_{\text{new}}(\beta, j|\mu), \quad (8)$$

which we put again into the process (P1') so that we can complete one iteration sequence.

We summarize the algorithm of the PWFRG for 1D quantum system as follows:

- Step 0. Prepare an input wavefunction Ψ_{old} and an associated initial projection matrix R_{old} . Choice of the initial Ψ_{old} is somewhat arbitrary; the exact ground-state wavefunction for a small-size system is conveniently chosen. Diagonalize the wavefunction matrix to obtain the initial projection matrix $\{R_{\text{old}}(\mu|i, \alpha)\}$.

Step 1. Apply the modified Lanczos operation \hat{L} to Ψ_{old} to obtain the improved wave function Ψ_{imp} . The operation $\hat{L} = \hat{L}(\alpha)$ on a state vector $|\Psi\rangle$ is defined as

$$\begin{aligned}\hat{L}(\alpha)|\Psi\rangle &= \frac{|\Psi\rangle + \alpha|\chi\rangle}{\sqrt{1 + \alpha^2 \langle \chi|\chi\rangle}} \\ &\equiv |\tilde{\Psi}(\alpha)\rangle \\ |\chi\rangle &\equiv \Delta H|\Psi\rangle \\ \Delta H &\equiv H - \langle \Psi|H|\Psi\rangle.\end{aligned}\quad (9)$$

The optimum choice $\alpha = \alpha^*$ minimizing $\langle \tilde{\Psi}(\alpha)|H|\tilde{\Psi}(\alpha)\rangle$ is given by

$$\begin{aligned}\alpha^* &= \left(\chi_3 - \sqrt{\chi_3^2 + 4\chi_2^3}\right)/(2\chi_2^2) \\ \chi_n &\equiv \langle \Psi|(\Delta H)^n|\Psi\rangle.\end{aligned}\quad (10)$$

Write $\hat{L}(\alpha^*)$ as \hat{L}^* . In most cases we adopt k -fold operation with $k \geq 2$:

$$\begin{aligned}|\Psi_{\text{imp}}\rangle &= [\hat{L}^*]^k |\Psi_{\text{old}}\rangle \\ &= \hat{L}^*(\hat{L}^*(\dots(\hat{L}^*|\Psi_{\text{old}}\rangle)\dots)) \quad (k \text{ times}).\end{aligned}\quad (11)$$

Step 2. Perform an eigenvalue decomposition of the wavefunction matrix $\{\hat{\Psi}_{\text{imp}}(\alpha, i|\beta, j)\}$ associated with the improved state vector $|\Psi_{\text{imp}}\rangle$:

$$\hat{\Psi}_{\text{imp}}(\alpha, i|\beta, j) = \sum_{\mu} A(\alpha, i|\mu) \omega_{\mu} A(\beta, j|\mu), \quad (12)$$

where the new block index μ ($= 1, 2, \dots$) is introduced in descending order of $|\omega_{\mu}|$ ($|\omega_1| \geq |\omega_2| \geq \dots$). We then truncate the number of retained bases to m .

Step 3. Extend the system size by adding two sites at the center of the chain. Then using the “refined” projection matrix $\{A(\alpha, i|\mu)\}$ ($\mu = 1, 2, \dots, m$), update the left and right block Hamiltonian matrix just as in the DMRG.

Step 4. Update the projection matrix following eq.(7) and form the new wavefunction Ψ_{new} according to eq.(8). Rename Ψ_{new} as Ψ_{old} , then go to Step 1.

After repeating the above steps sufficiently many times, we obtain the “fixed point” wavefunction. Physical quantities are calculated as the expectation value with respect to the fixed-point wavefunction. In particular, the per-site magnetization M is calculated as the expectation value of the center spins.

Let us give a comment on the relation between the PWFRG and the DMRG. As regards the diagonalization of the wavefunction matrix, a similar process (singular-value decomposition, SVD for short) appears in the original DMRG [2]. The associated projection matrix R is an important object in both methods. Main difference in the two methods lies in the updation process of R . In the DMRG, the updation $R_{\text{old}} \rightarrow R_{\text{new}}$ is “directly” given by the SVD of the updated ground-state wavefunction of the updated Hamiltonian matrix. Whereas, in the PWFRG, the updation is given somewhat “indirectly” through the recursion relation eq.(7). We *do not* determine R_{new} from the updated wavefunction, but we *define* R_{new} by eq.(7) and use it to *form* the updated wavefunction. The updated wavefunction is, then, a good guess of the ground-state wavefunction of the system with the extended size (by two sites). We then refine the wavefunction by the modified Lanczos operation eq.(9) to obtain the “refined projection matrix” A . As the iteration proceeds, the system size becomes larger and larger, and *at the same time*, the wavefunction becomes closer and closer to the ground-state wavefunction. The recursion relation eq.(7) implies that, at the fixed point (=infinite iterations), $R = A$ should be satisfied, and this is precisely the condition for the ground-state wavefunction which must be invariant under the modified Lanczos operation.

We apply the PWFRG to several models of quantum spin chains to draw the zero-temperature $M-H$ curves. We present the results in the followings.

(a) $S = 1/2$ XY antiferromagnetic chain [12, 13]

The local Hamiltonian h (see eq.(1)) for this model is given by

$$h(\vec{s}_i, \vec{s}_j) = |J|(s_i^x s_j^x + s_i^y s_j^y), \quad (13)$$

with \vec{s}_i being $\frac{1}{2} \times$ (Pauli spin matrices). This model is exactly soluble via the Jordan-Wigner transformation; the magnetization curve is known to be

$$M = \frac{1}{\pi} \sin^{-1}\left(\frac{H}{|J|}\right). \quad (14)$$

This model is a gapless system even at $H = 0$, which is reflected in the behavior of the $M-H$ curve: $\lim_{M \rightarrow 0^+} H(M) = 0$. In Fig. 1 we compare the PWFRG calculation with the exact solution, where an excellent agreement is seen. It should be noted that even a small number ($m = 16$) of retained bases gives the quite accurate $M-H$ curve.

(b) Takhtajan-Babujian model [14, 15] ($S = 1$)

This model belongs to a family of models called bilinear-biquadratic chains whose local Hamiltonians have the form

$$h(\vec{s}_i, \vec{s}_j) = |J|[\vec{s}_i \cdot \vec{s}_j + \tilde{\beta}(\vec{s}_i \cdot \vec{s}_j)^2], \quad (15)$$

where \vec{s}_i and \vec{s}_j are $S = 1$ spin operators. The Takhtajan-Babujian model corresponds to $\tilde{\beta} = -1$, which is exactly soluble and is known to be gapless [14, 15]. The $M-H$ curve can be drawn by solving the Bethe ansatz integral equation for the “two-string” (two-down-spin bound state) root density to obtain the ground-state energy density with fixed per-site magnetization M . For general M the solution can only be obtained numerically, by converting the integral equation into a matrix equation. As can be seen in Fig. 2, our PWFRG calculation reproduces the exact curve within a satisfactory precision even with the small number m ($= 20$) of the retained bases.

(c) Affleck-Kennedy-Lieb-Tasaki (AKLT) chain [16] ($S = 1$)

This model also belongs to the family of the $S = 1$ bilinear-biquadratic chains, whose local Hamiltonian being given by eq.(15) with $\tilde{\beta} = 1/3$. The ground state at $H = 0$ is exactly known to be singlet and gapped (the excitation gap $\Delta > 0$), and is in the “valence bond solid” (VBS) state whose wavefunction is the product of matrices with finite dimensions [17, 18]. The ground-state correlation length and the string order-parameter are also exactly known, from which the state is identified to be in the “Haldane phase” [19]. Increasing the magnetic field H , this VBS state remains to be the ground state up to the “lower critical field” H_{c1} above which the ground state is magnetized. The critical field relates to the gap Δ as

$$H_{c1} = \Delta, \quad (16)$$

which holds for a general class of antiferromagnets so long as Δ is the singlet-to-triplet energy gap. There is another critical field H_{c2} (upper critical

field) above which the system's per-site magnetization saturates to unity (complete ferromagnetic state). For the intermediate region of the field, $H_{c1} < H < H_{c2}$, the exact ground-state wavefunction has not been known even for the AKLT chain. It should be noted that the VBS-state wavefunction [16, 17, 18] with finite matrix size m ($m = 2$ for the AKLT chain) is exactly the fixed point of the iterations in the DMRG/PWFRG with the number of retained bases just being m [20]. Hence, by continuity, we can expect that the fixed-point wavefunction of the DMRG/PWFRG with relatively small m should remain to be a good approximation to the correct ground-state wavefunction of the AKLT chain even in the intermediate range of the field.

In Fig. 3 we draw the $M - H$ curve obtained by the PWFRG with a small number m ($= 20$) of the retained bases. The calculation reproduces the exact value of $H_{c2} = 4|J|$ which can be derived from the stability consideration of the saturated state against the one down-spin formation [21, 23, 22]. Further, the predicted square-root behavior [21, 23, 22]

$$M(H) \sim S - A_2 \sqrt{H_{c2} - H} \quad ((0 <) A_2 : \text{constant}) \quad (17)$$

is reproduced (Fig. 4).

As for the behavior near the lower critical field H_{c1} , another square-root behavior has been expected [24, 25, 26, 27]:

$$\begin{aligned} M(H) &\sim A_1 \sqrt{H - H_{c1}} \quad ((0 <) A_1 : \text{constant}), \\ H_{c1} &= \Delta. \end{aligned} \quad (18)$$

Although actual studies concerning this behavior have been almost limited to the case of the "pure" $S = 1$ Heisenberg chain without the biquadratic term ($\tilde{\beta} = 0$ in eq.(15)), the theoretical arguments for this behavior are so general that we can naturally expect the square-root behavior eq.(18) to hold for the AKLT chain either. As can be seen from Fig. 5, our PWFRG calculation is consistent with eq.(18); the calculated value of $H_{c1} \simeq 0.7|J|$ is in agreement with the previous numerical estimation of Δ [29, 28].

To summarize, in this article we have presented the application of the product-wavefunction renormalization-group (PWFRG) method [6] to quantum spin chains to draw the zero-temperature magnetization curve. The results show that the method works efficiently even for systems with finitely-magnetized ground states which are gapless.

We should give a comment on application of the DMRG to the magnetization process of quantum spin chains. In a preliminary stage of the present study, we adopted the original infinite-algorithm of the DMRG. We then found that the DMRG, applied to quantum antiferromagnets in the magnetized region, is very likely to be “trapped” by “metastable states”, leading typically to oscillatory behavior in the course of the iteration. As a result, in most cases, we failed in obtaining the magnetized ground-state wavefunction corresponding to the fixed point. In contrast, the PWFRG adopted in the present study is fairly stable, always successful in reaching the fixed point even in the magnetized region. The above “instability” of the DMRG is certainly related to the nature of the present problem. The magnetization curve reflects a continuous sequence of level-crossing transitions induced by varying magnetic field, between the states with different values of total S^z . The exact diagonalization (instead of the modified Lanczos operation used in the present study) in the original DMRG extracts the exact lowest energy state of the truncated Hamiltonian at each iteration step. The state is, however, the lowest energy state of the system at that size ($\sim 2 \times$ iteration steps); owing to the highly degenerate energy level structure, there may well occur “level crossings” on the increasing system size, leading to the oscillatory behavior in the iteration.

Of course, we can remove this instability by decomposing the state space into subspaces according to quantum numbers to reduce the degeneracy. For the problem of the magnetization process the quantum number is the total S^z ($\equiv S_T^z$) and we can surely perform the DMRG with fixed S_T^z . This approach, however, is rather laborious because what we need is the ground-state energy density with fixed magnetization *density* S_T^z/N (N : lattice size), which requires a huge number of fixed- S_T^z calculations ($S_T^z = 0, 1, 2, \dots, NS$, for the spin S case) for large N , to find the optimum value of S_T^z giving the true ground state under the field. On the other hand, with the PWFRG method, the system gradually and automatically converges into the “true” ground state under the given magnetic field. Due to this “stability”, the PWFRG will be particularly useful for “critical” systems whose energy spectrum (or transfer-matrix eigenvalue spectrum, for 2D classical systems) is highly degenerate.

The modified Lanczos method used in this article is a two-step restriction of the ordinary Lanczos algorithm. Similar restricted-step Lanczos has been also employed in a new version of the DMRG (finite-system algorithm) [35] which shows very high efficiency. Although precise relation between the PWFRG and the new DMRG is not obvious, we can say that the former

may, in a sense, be the infinite-system-algorithm version of the latter.

As for the magnetization process, the “middle-field” phase transitions to occur between H_{c1} and H_{c2} have been known for some systems [30, 31, 32]. Study of such field-induced ground-state phase transitions is an interesting future problem. Finite-temperature behavior [33, 34] of the magnetization process is also an interesting problem.

We would like to thank T. Nishino, M. Kikuchi, H. Kiwata and R. Sato for valuable discussions. This work was partially supported by the Grant-in-Aid for Scientific Research from Ministry of Education, Science, Sports and Culture (No.07640514). A part of the numerical computation was made on the system VPP500 of the Supercomputer Center, Institute for Solid State Physics, the University of Tokyo. One of us (K.O) is supported by JSPS Research Fellowships for Young Scientists.

References

- [1] M.N. Barber: in *Phase Transitions and Critical Phenomena*, Vol. 8, eds. C. Domb and J.L. Lebowitz (Academic Press, New York, 1983) p. 146, and references therein.
- [2] S.R. White: Phys. Rev. Lett. **69** (1992) 2863; Phys. Rev. **B 48** (1993) 10345.
- [3] T. Nishino: J. Phys. Soc. Jpn. **64** (1995) 3598.
- [4] T. Nishino and K. Okunishi: J. Phys. Soc. Jpn. **65** (1996) 891.
- [5] T. Nishino, K. Okunishi and M. Kikuchi: Phys. Lett. **A 213** (1996) 69.
- [6] T. Nishino and K. Okunishi: J. Phys. Soc. Jpn. **64** (1995) 4084.
- [7] R. J. Baxter: J. Math. Phys. **9** (1968) 650; J. Stat. Phys. **19** (1978) 461; *Exactly Solved Models in Statistical Mechanics* (Academic Press, London, 1982).
- [8] K. Katsumata, H. Hori, T. Takeuchi, M. Date, A. Yamagishi and J. P. Renard: Phys. Rev. Lett. **63** (1989) 86.
- [9] Y. Ajiro, T. Goto, H. Kikuchi, T. Sakakibara and T. Inami: Phys. Rev. Lett. **63** (1989) 1424.
- [10] E. R. Davidson: J. Comput. Phys. **17** (1975) 87.

- [11] T. Z. Kalamboukis: J. Phys. A **13** (1980) 57.
- [12] E. Lieb, T.Schultz and D. Mattis : Ann. Phys. **16** (1961) 407.
- [13] S. Katsura : Phys. Rev. **127** (1962) 1508, **129** (1963) 2835.
- [14] L.A. Takhtajan: Phys. Lett. **A 87** (1982) 479.
- [15] H.M. Babujian: Phys. Lett. **A 90** (1982) 479; Nucl. Phys. **B 215** (1983) 317.
- [16] I. Affleck, T. Kennedy, E. H. Lieb and H. Tasaki: Phys. Rev. Lett. **59** (1987) 799; Commun. Math. Phys. **115** (1988) 477.
- [17] A. Klümper, A. Schadschneider and J. Zittartz: Z. Phys. **B87** (1992) 281; Europhys. Lett. **24** (1993) 293.
- [18] A. Schadschneider and J. Zittartz: Ann. Physik **4** (1995) 157.
- [19] F.D.M. Haldane: Phys. Lett. **93A** (1983) 464; Phys. Rev. Lett. **50** (1983) 1153.
- [20] S. Östlund and S. Rommer: Phys. Rev. Lett **75** (1995) 3537; preprint, cond-mat/9606213.
- [21] J. B. Parkinson and J. C. Bonner: Phys. Rev. B **32** (1985) 4703.
- [22] R. P. Hodgson and J. B. Parkinson: J.Phys.C:Solid State Phys. **18** (1985) 6385.
- [23] H.Kiwata and Y.Akutsu: J. Phys. Soc. Jpn **63** (1994) 3598.
- [24] I.Affleck: Phys. Rev. B **43** (1991) 3215.
- [25] A.M.Tsvelik: Phys. Rev. B **42** (1990) 10499.
- [26] M.Takahashi and T.Sakai: J. Phys. Soc. Jpn **60** (1991) 760.
- [27] E.S.Sørensen and I.Affleck: Phys. Rev. Lett. **71** (1993) 1633.
- [28] G. Fáth and J. Sólyom: J.Phys.:Condens Matter **5** (1993) 8983.
- [29] U. Schollwöck, Th. Jolicoeur and T. Garel: Phys. Rev. B **53** (1996) 3304.
- [30] J. B. Parkinson : J.Phys.:Condens Matter **1** (1989) 6709.

- [31] H. Kiwata and Y. Akutsu: J. Phys. Soc. Jpn **63** (1994) 4269.
- [32] R. Sato and Y. Akutsu: J. Phys. Soc. Jpn **65** (1996) 1885.
- [33] S. Yamamoto and S. Miyashita: Phys. Rev. B **51** (1995) 3649.
- [34] R. J. Bursill and T. Xiang and G. A. Gehring: J. Phys.: Condens Matter **8** (1996) L1.
- [35] S. R. White: Phys. Rev. Lett. **77** (1996) 3633.

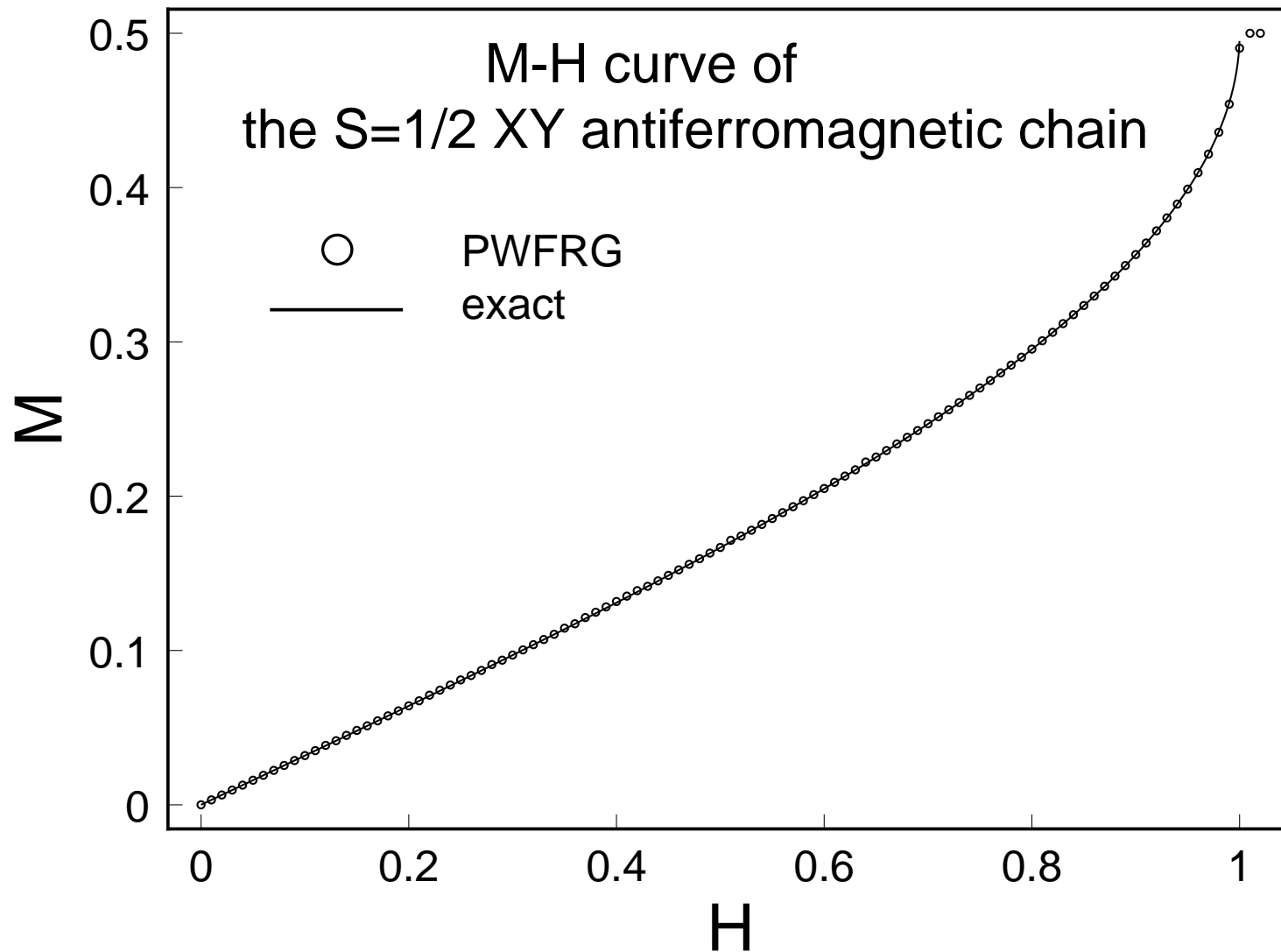
Figure 1: $M - H$ curve of the $S = 1/2$ XY antiferromagnetic chain.

Figure 2: $M - H$ curve of the Takhtajan-Babujian model.

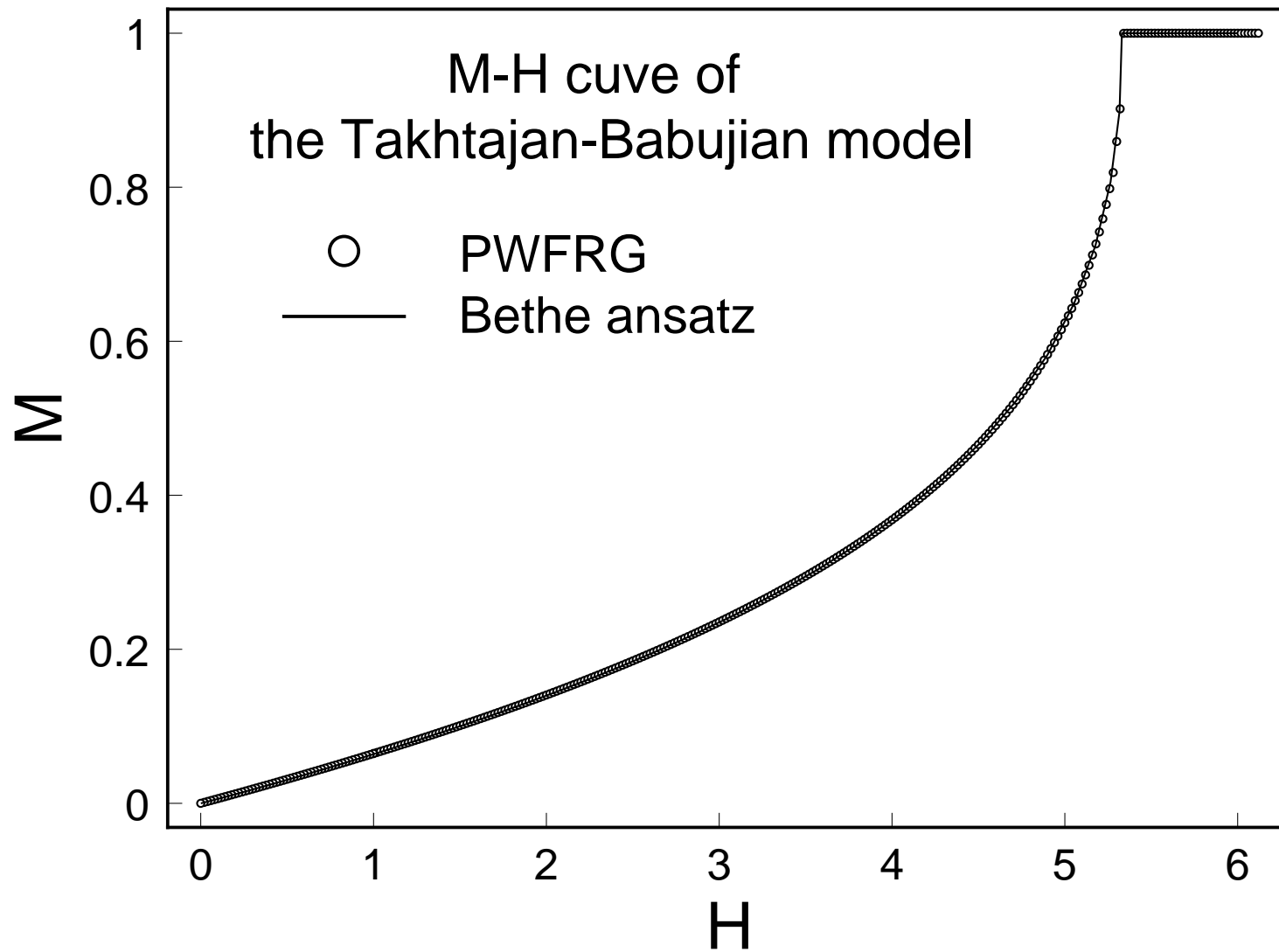
Figure 3: $M - H$ curve of the Affleck-Kennedy-Lieb-Tasaki chain.

Figure 4: The magnetization curve of the Affleck-Kennedy-Lieb-Tasaki chain near the saturation field H_{c2} .

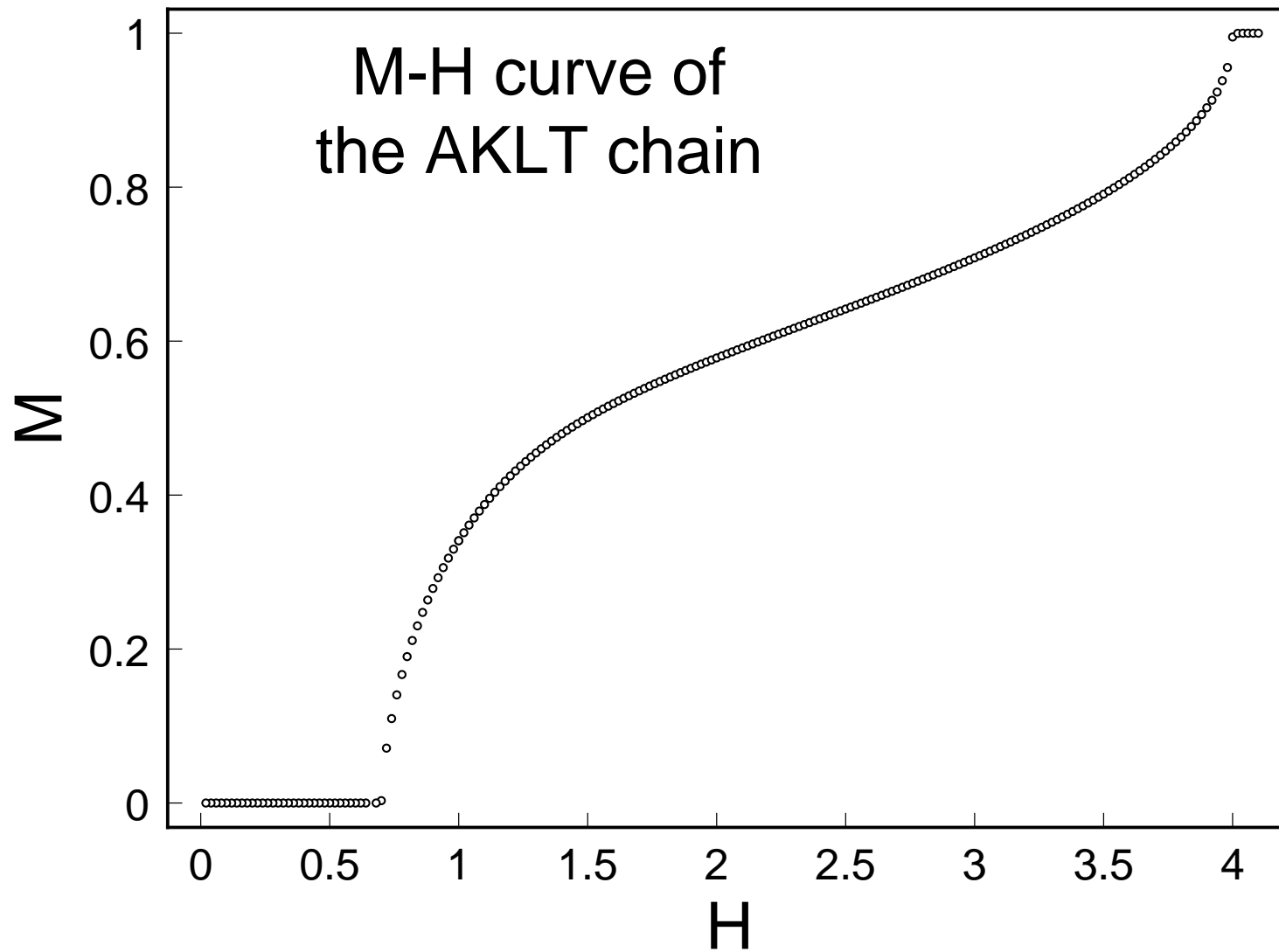
Figure 5: The magnetization curve of the Affleck-Kennedy-Lieb-Tasaki chain near the lower critical field H_{c1} .



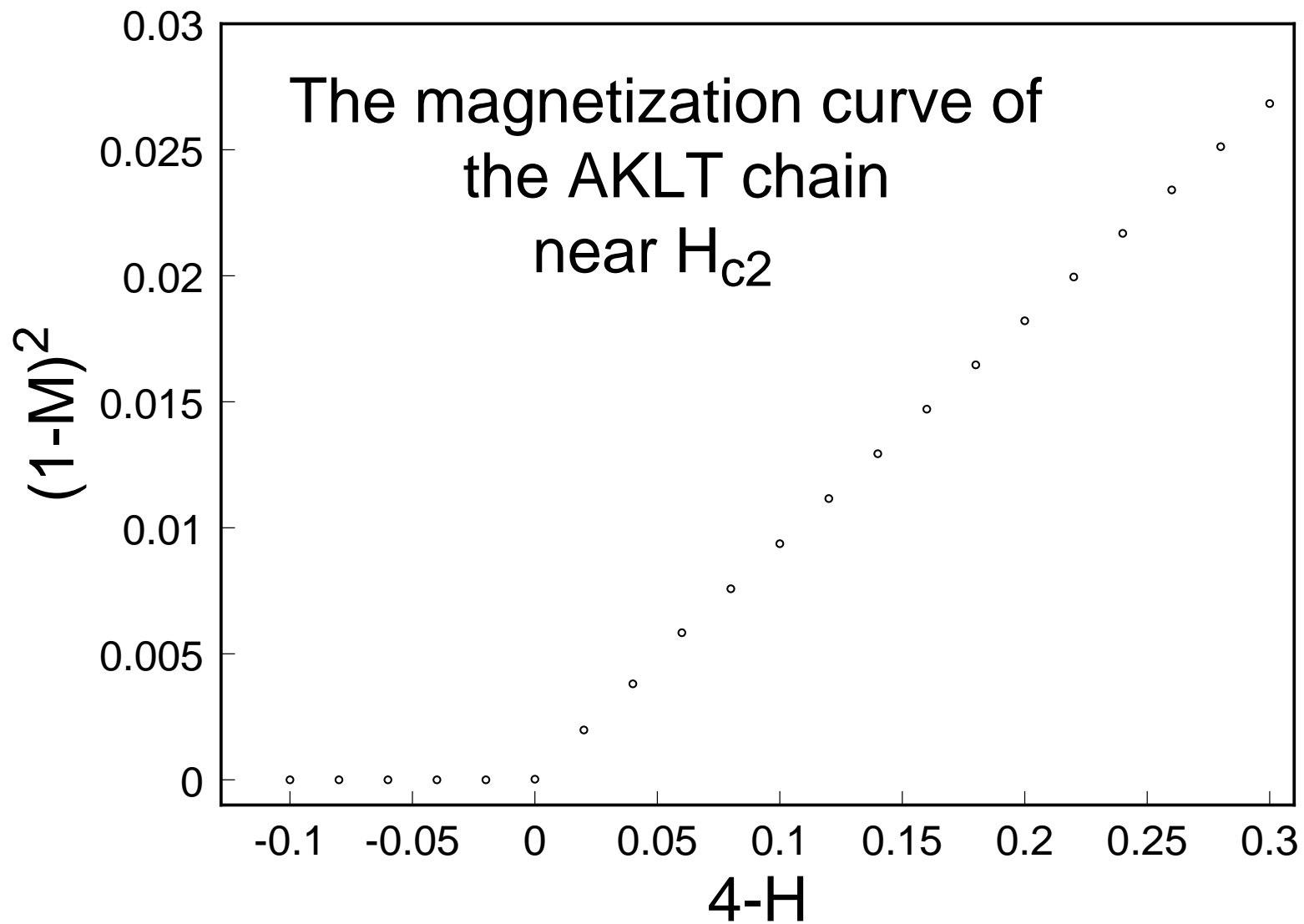
Y. Hieida, K. Okunishi, Y. Akutsu, Fig.1



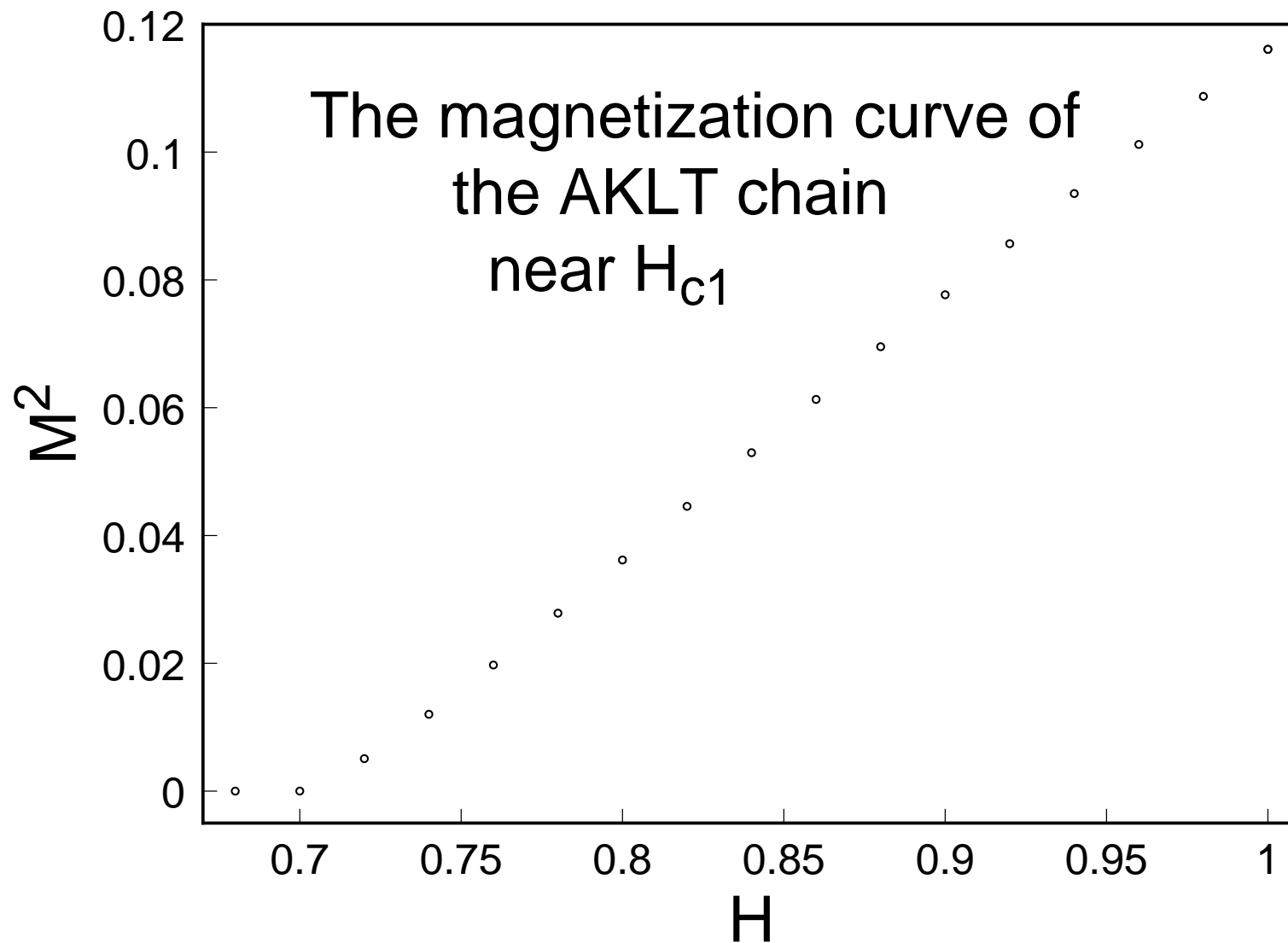
Y. Hieida, K. Okunishi, Y. Akutsu, Fig.2



Y. Hieida, K. Okunishi, Y. Akutsu Fig.3



Y. Hieida, K. Okunishi, Y. Akutsu Fig.4



Y. Hieida, K. Okunishi, Y. Akutsu Fig.5